Measurement and Computational Modeling of Radio-Frequency Electromagnetic Power Density Around GSM Base Transceiver Station Antennas

P. Nassiri[1], M. Saviz[2], M. Helmi-kohnehShahri[1*], M. Pourhosein[1], R. Divani[1]

[1] Department of Occupational Health Engineering, School of Public Health, Tehran University of Medical Sciences, Tehran, Iran
[2] Department of Biomedical Engineering, Amirkabir University of Technology, Tehran, Iran

ABSTRACT: Evaluating the power densities emitted by GSM1800 and GSM900 BTS antennas is conducted via two methods. Measurements are carried out in half a square meter grids around two antennas. CST Microwave STUDIO software is employed to estimate the power densities in order for detailed antenna and tower modeling and simulation of power density. Finally, measurements obtained from computational and experimental methods were compared through the contour lines using the statistical Surfer software. After measuring and simulating all values, it turns out that power density is generally lower than the permissible exposure limits although exceeds the limits in some sample points. According to the measurements, simulation error in stations GSM900 and GSM1800 are 10% and 8%, respectively. Findings from contour-line-maps illustrates that direct measurement method follows the same emission pattern as the computational method does. It validates the computational approach and the models attained for BTS power density estimation.

1- Introduction

Radiofrequency waves include electromagnetic waves that have frequencies from 3 kHz to 300 GHz. These waves are often used for telecommunications, radars, satellites, etc. [1]. The use of mobile phones involves frequencies from multiple hundred MHz to several GHz. Since 1980, the Global System for Mobile (GSM) communications has rapidly grown, and the increased demand in global markets has made GSM900/1800 the most popular antennas [2, 3], being widely used throughout the country despite the advent of newer technologies. Since the rise in utilization rates of cellular mobile phones, human health concerns have also increased with regard to the exposure of residents in the vicinity of base transceiver stations (BTS) and related towers to radiofrequency waves and microwaves. Most of the antennas are mounted on masts and at the top of buildings in residential areas; therefore, people might become exposed to radiation. [4-5]. If body organs experience prolonged exposure to microwaves, they are affected by the absorbed energy. If the body fails to compensate for the effects and is unable to return to the normal situation, many organs can get damaged [6]. Adverse effects of microwaves are classified into thermal and non-thermal classes. Thermal effects are caused by the wave-induced temperature rise. Cataract, skin burn, and taste-sense damages are some of the adverse thermal effects of microwaves. In addition, various studies have considered non-thermal effects of microwaves, namely reproductive cells, cancers, mental effects and oxidative changes as well as changes in the stimulation pattern of nerve cells while many other undiscovered aspects remain [7-8].

International Commission on Non-Ionizing Radiation Protection (ICNIRP) has determined the permissible occupational exposure to electromagnetic waves and the minimum health and safety requirements in form of directive EC/40/2004. This directive does not cover chronic or prolonged exposure side effects, e.g. cancer; however, it controls well-known short-term and severe side effects [2-4-7]. Despite such limitations, it is cited, and used by radio regulation agencies in a majority of countries. In order to verify compliance with restrictions set by these standards, size estimation of the radiation fields is required; however, due to some reasons, for example the heights of the antennas, measuring the electromagnetic waves around the BTS antennas and masts are sometimes costly [7-8-9]. Furthermore, the measuring of the electromagnetic fields inside the body as a standard basic quantity, which should not exceed the permissible limits, is practically impossible [10-12]. Simulation of models is increasingly used to solve problems and make effective decisions [13]. Numerical models can be helpful in assessing the electromagnetic fields around the antennas [14]. Modeling, in fact, can give information about the safe distance from antenna especially in cases where it is impossible to do the direct measurement, such as the estimation of fields inside the body [1, 5, 13].

The present study is aimed at discussing the applications of both methods of direct measurement and computational simulation in order to estimate the exposure to emitted waves from BTS antennas. Once the numerical data obtained from simulation are validated in comparison with measurements, simulation can be applied for the estimation of fields inside the body which are often impossible to measure. Since for the application of safety standards with basic restrictions, the fields inside the body should be estimated, and due to the fact that simulation is the only way to apply this scenario, it is important to ascertain the applicability of computational simulation models for this purpose. To begin with, methods

The corresponding author; Email: m-helmi@alumnus.tums.ac.ir

of simulation for computing the fields outside the body, that are easy to measure, and comparing them with the results of measurements and validating them are the subject of this paper. Furthermore, the exposure values obtained and reference limits (permissible incident fields on the body cited by radiation protection standards) were compared to obtain an estimation of permissible distances from the antenna.

2- Materials and Methods

This paper studies the waves captured around the two real BTS antennas: GSM 900MHz and GSM 1800MHz panel antennas. Both antennas were mounted on the roofs of buildings. The surface density of radiated power was measured and simulated over coordinated grids around the masts.

2- 1- Power density around BTS antennas

The most common way of characterizing the antenna's emitted power density is to measure the radiated power density in the far field region by choosing a source receiver antenna and taking some samples from radiation properties at different points around the antenna with a spectrum analyzer. Only one signal path between the receiver and source antennas should exist in order to measure the radiation properties of the antenna without the scattering effects from adjacent objects. This situation can be created by an anechoic chamber which has minimal reflection from the surrounding walls similar to the free space conditions. However, assessing a mast antenna radiation is not possible within most normal anechoic chambers and is an objective field survey which can be performed by dividing the environment into certain dimension grids around the antenna.

To measure the power densities around the BTS mast antennas in situ, the studied area was divided into grids, where each unit-cell had an area of 0.5 m2. Power density was measured using a calibrated spectrometer SPECTRAN RF 4060 at the height of 1.6 m from the center of grid-cells. In each point, measurements were taken in one minute and all data and coordinate references were recorded in order to compare the corresponding power density values with simulation models. 64 points around the GSM1800 antenna and 156 points around the GSM900 antenna were selected. However, field perturbations are expected due to reflections from e.g. metallic objects at grid points close to such structures. Spot measurements were done for all grid centers in which 9 points and 19 points in GSM1800 and GSM900 stations, respectively, were excluded from measurements due to proximity to metallic objects and probable dominance of reflections.

2- 2- Modeling antennas and simulating power density around the masts

2- 2- 1- Modeling antennas

A BST antenna contains mast and panel. Modeled antennas for GSM900 and GSM1800 stations are an aluminum guyed mast type G55 having the height of 2.7 m and an aluminum guyed mast type G45 with the height 2.2 m, respectively. The panel of the antenna consists of a reflector, sector, and fiberglass cover (Figure 1).

Panel reflector, made of aluminum, is a reflector of backward waves. Sector or radiator has three main sections of dipoles, holder, and reflector. Figure 1 shows the dipoles and holder.

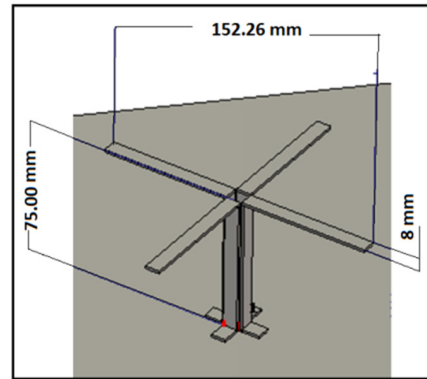**Fig. 1. Internal structure of Panel GSM900**
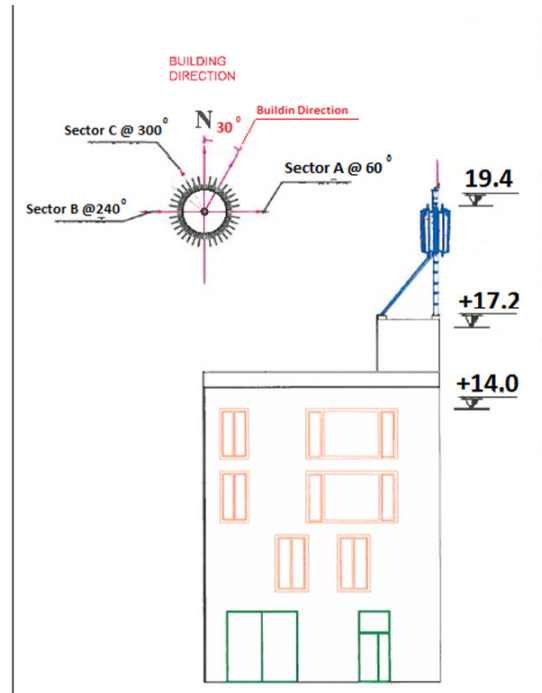

Fig. 2. Model for Antenna GSM

Fig. 3.GSM900 antenna station [15]

Initial value for the dipoles was set half a wavelength. Finally, by assembling the sections, a model for BTS antenna is created. The following information was extracted from the studied antenna's catalog:

Station 1: KATHREIN A-Panel GSM900- Dual polarization antenna, having the dual polarity of +45°/-45°, frequency band of 806-960, impedance of 50 Ohms, excitation power of 12 W, and dimensions of 116, 262,1296 mm for thickness, width, and height, respectively (Figure 3).

Station 2: KATHREIN F-PanelGSM1800- Dual polarization

antenna, having the dual polarity of +45°/-45°, frequency band of 1710-1880, impedance of 50 Ohms, excitation power of 12 W, and dimensions of 702, 155, 602 mm for thickness, width, and height, respectively.
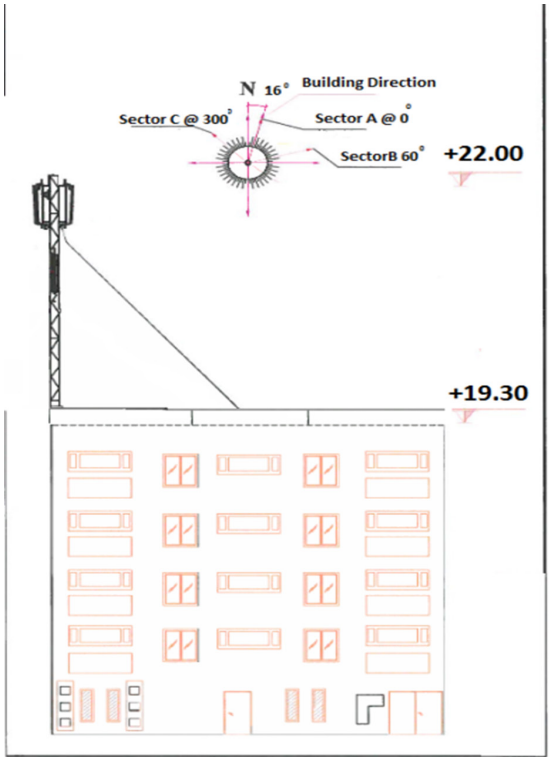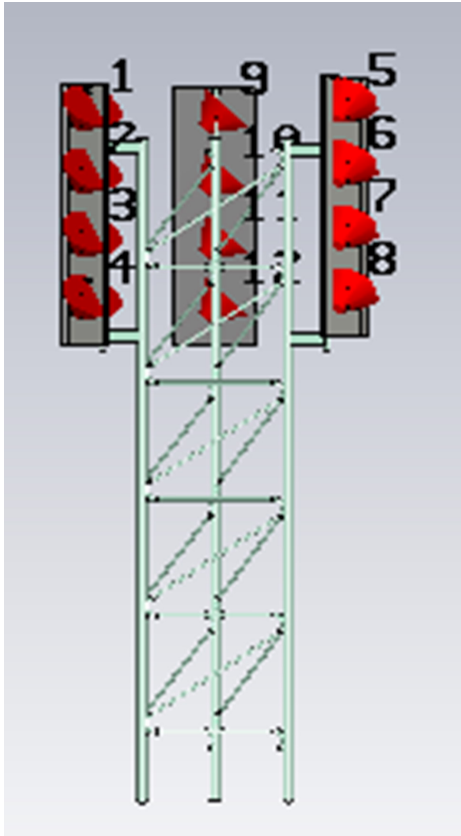

Fig. 4.GSM1800 antenna station [16]

Fig. 5. Mast modeled from for Antenna GSM1800

Finally, the models of antennas and masts were made using CST Microwave STUDIO software considering the fact that the power of antenna changes under different conditions. In all results from simulation and direct measurements, obtained values will be normalized to the average value of power density.

2- 2- 2- Power density simulation

The surface power density is theoretically obtained as the magnitude of the poynting vector, which is computed through a cross-product of electric and magnetic field vectors:

$$\vec{S}(x,y,z;t) = \vec{E}(x,y,z;t) \times \vec{H}(x,y,z;t) \tag{1}$$

Vectors E and H represent the instantaneous electric field and instantaneous magnetic field intensities, respectively. The average poynting vector in the time domain is equal to the average power density and is the real part of the Poynting's vector in the frequency domain.

$$\overrightarrow{S(x,y,z;t)} = Re\left\{ \frac{1}{2}\vec{E}(x,y,z;\omega) \times \overrightarrow{H}^{*}(x,y,z;\omega) \right\} \tag{2}$$

ω : is the angular frequency of operation
E: is the electric field;
B: is the magnetic field.
* :denotes the complex conjugate
Re: Real Part of a complex number
For simulations, the Finite Integration Technique solver (FIT) from the Computer Simulation Technology (CST) software was employed. The methodology of FIT is similar to FDTD, and both are based on the Finite Difference Method (FDT) in both time and space; however, they were solved using the integral forms in Maxwell's equations as follows:

$$\oiint_{\partial A} \vec{E}.d\vec{s} = -\int_{A} \frac{\partial \vec{B}}{\partial t}.d\vec{A} \tag{3}$$

$$\oiint_{\partial A} \vec{H}.d\vec{s} = \int_{A} \left(\frac{\partial \vec{D}}{\partial t} + \vec{j} \right).d\vec{A} \tag{4}$$

$$\oiint_{\partial V} \overrightarrow{D}.d\vec{A} = \int_{V} \rho.dV \tag{5}$$

$$\oiint_{\partial V} \vec{B}.d\vec{A} = 0 \tag{6}$$

For numerical calculations in these equations, the calculation domain should be discretized corresponding to the measurement grid. GSM900 and GSM1800 antenna stations with dimensions 7×6 m^2 (Figure 6) and 4×4 m^2 (Figure 7), respectively were divided into 0.5-m^2 grids and the average power density is computed on a spot at the height of 1.6 m from the center of each grid.

In this study, the computational domain for numerical calculations around the BTS mast antenna is selected by considering coordinates of the farthest measurement point. In addition, the maximum efficiency is obtained by the hexagonal meshing on a 48GB RAM system. The number of mesh cells and the time required for simulation were obtained as 824, 326, 010, 1-78 and 840, 143, 459, 1-83 hours for GSM 900 and GSM1800 stations, respectively. Results are then extracted for the power density at the same location as those used for

measurements. ICNIRP standard reference limits were used to assess the safe distances for each of these two methods. The reference limits indicate the permissible limitations of incident radiation fields (the field in a person's hypothetical location before their actual presence). The reference limits are found by high-confidence intervals such that the basic restrictions that state the permissible field strengths inside the body are met. According to the ICNIRP standards, over the frequency range of 2000-4000 MHz, the permissible occupational exposure limits are calculated by placing f (in MHz) in f/40 and f/200 to calculate the occupational power density and public exposure limits, respectively. Note that permissible occupational exposure limits are often higher than the permissible public exposure limits; this is because of the assumption that the public is more vulnerable than occupational groups. In fact, the occupational exposure means power density limitations that if exceeded, adverse effects on worker's body are expected [12]. Considering the central frequencies of the surveyed antennas, the permissible occupational and environmental exposure limits are obtained as 22.5 W/M^2 and 4.5 W /M2 for GSM900 and 45 W/M2 and 9 W/M^2 for GSM1800, respectively. Finally, results were graphically assessed. In order to do graphical assessments, results were converted into contour maps (contour lines) and the maps were overlaid. A contour line of the function of two variables is a curve Along the function which has a constant value. It is a cross-section of the three-dimensional graph of the function f(x, y) parallel to the x, y plane. In cartography, a contour line joins points with equal heights. The contour lines shown in Figures 12 to 14 join points with equal power densities.

3- Results

3- 1- Measurement of surface power density
Figures 6 and 7 show the Gridding area around the masts and the obtained power densities around the two antennas. Power density at different grid points was obtained by measuring the mean power density at those points distancing from the antenna. The two stations are quite similar in dimensions but due to the blind spots in the measurement, the number of measurement grids is less than the one in the simulation Table 1 demonstrates the statistical properties of the both studied stations. The variation ranges of the measured values around GSM900 and GSM1800 were 4.6W/m^2 and 8.9W/m^2, respectively Findings show that both the stations have a descending pattern by distancing from the antenna.

3- 2- Power density simulation results
Modeling was done based on the antenna, mast and environmental properties using CST software. Power density was then simulated to find X, Y, and Z components by computer and the average power density was obtained from the sum of three power densities on three coordinates. Results obtained from power density simulation of GSM900 and GSM1800 antenna stations are presented in Figures 8 and 9. The simulation is conducted based on the co-ordinates of measurement and non-measured grids which are excluded from the study. Table 2 shows the stations' statistical properties.

4- Discussion
According to the present study, it can be stated that there is eight

to ten per cent difference between measurement and simulation values in GSM900 and GSM1800 stations. This difference can be due to the impact of reflectance distributions, antenna power changes, measurement method, etc. Comparing with ICNIRP standards, most obtained power density values were obviously lower than the required occupational exposure limits; however, one grid point in GSM900 antenna station and two grid points in GSM1800 antenna station (with the distance of 75cm from the front, and the height of 60 cm below the antenna) exceeded the required environmental exposure limits. Upon comparing the statistics of measured and simulated results in Tables 1 and 2, one can see that the central indices and variances of the measured values are high.
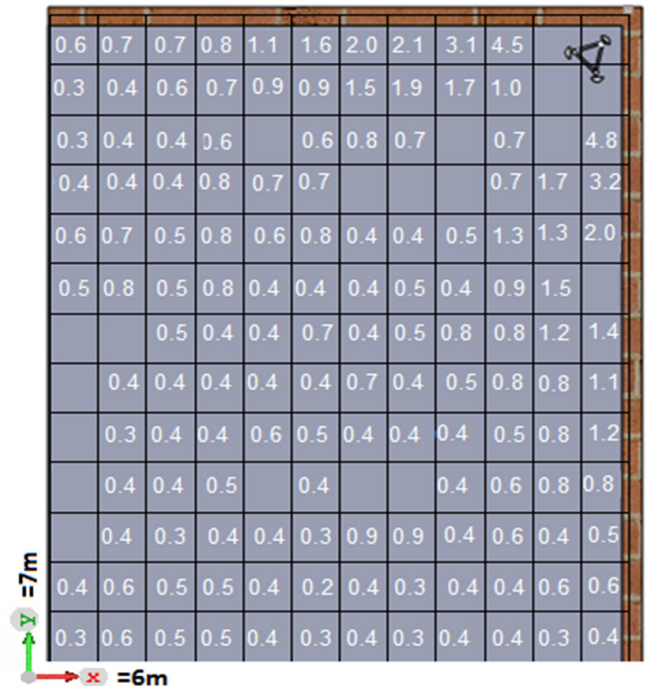

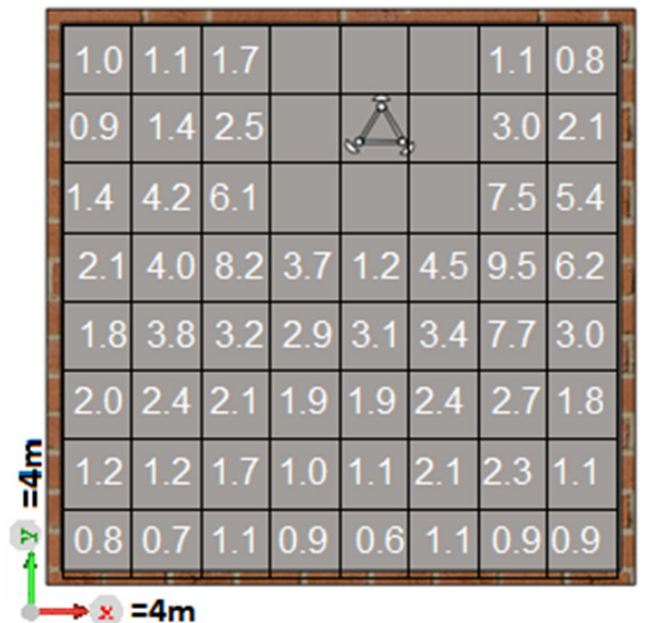**Fig. 6. Measurement of mean power density in 156 points around the GSM900 antenna at height of 1.6 m from roof-ground.**

Fig. 7. Measurement of mean power density in 64 points around the GSM 1800 antenna at height of 1.6 m from the roof-ground.

Table 1. Statistical Properties of measured power density distribution (W/m²) around the two stations

	Power density (w/m²)	
	station GSM1800	station GSM900
Minimum	0.6	0.2
Maximum	9.5	4.8
25%-tile	1.1	0.4
75%-tile	3.1	0.8
Median	1.8	0.5
Range	8.9	4.6
Mean	2.62	0.7
Standard Deviation	2.07	0.66
Variance	4.3	0.43

Table 2. Results of Statistical properties from the power density (W/m²) simulation around the antennas

	Power density (w/m²)	
	station GSM1800	station GSM900
Minimum	0.6	0.1
Maximum	10.6	0.7
25%-tile	1.25	0.3
75%-tile	3.74	0.7
Median	2	0.5
Range	2.6	4.2
Mean	2.6	0.63
Standard Deviation	2.05	0.56
Variance	4.2	0.31

0.7	0.6	0.5	0.8	1.3	1.6	1.8	1.4	3.3	4.3	0	0
0.5	0.4	0.4	0.3	0.9	1.1	1.3	1.2	1.9	0.6	0	0
0.5	0.4	0.3	0.3	0.7	0.6	0.9	0.5	0.3	0.9	1.2	1.4
0.7	0.5	0.3	0.3	0.5	0.7	0.4	0.3	0.3	0.7	1.9	2.9
0.4	0.5	0.5	0.3	0.4	0.6	0.4	0.4	0.3	0.5	0.7	1.5
0.6	0.4	0.5	0.1	0.6	0.3	0.4	0.6	0.3	1.3	1.3	1.6
0.3	0.2	0.3	0.2	0.3	0.3	0.6	0.5	0.6	0.6	1.4	1.9
0.2	0.3	0.2	0.4	0.4	0.3	0.3	0.2	0.4	0.3	0.7	1.2
0.2	0.6	0.3	0.6	0.4	0.2	0.1	0.3	0.4	0.3	0.4	0.9
0.5	0.8	0.6	0.5	0.4	0.3	0.1	0.2	0.4	0.4	0.3	0.5
0.8	0.8	0.7	0.5	0.4	0.2	0.2	0.3	0.5	0.5	0.4	0.5
0.1	0.9	0.6	0.3	0.8	0.1	0.4	0.4	0.7	0.6	0.5	0.6
0.6	0.6	0.7	0.2	0.2	0.3	0.5	0.6	0.7	0.6	0.6	0.7

Fig. 8. Simulated Average power densities (W/m²) around the GSM900 antenna

0.9	1.5	1.9				1.3	0.6
1.0	2.6	2.4				2.8	2.0
1.2	4.3	6.3				5.2	6.1
1.8	3.8	8.9	3.6	1.8	4.1	10.6	5.8
1.7	3.4	3.5	2.7	3.7	4.4	6.7	2.9
1.8	2.3	2.3	2.0	1.8	2.4	2.5	1.7
1.4	1.5	1.4	1.2	1.1	2.2	2.2	1.0
1.0	0.9	1.1	0.9	0.7	1.2	0.9	1.9

Fig. 9. Simulated average power densities (W/m²) around GSM1800 antenna
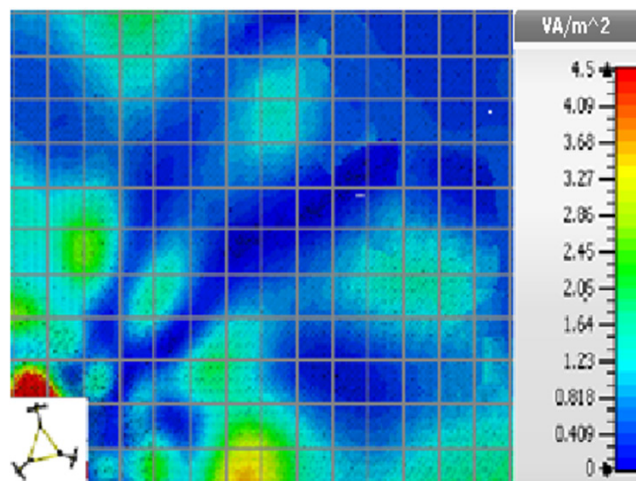

Fig. 10. Determination of safe distance in GSM900 station based on environmental and occupational exposure limits
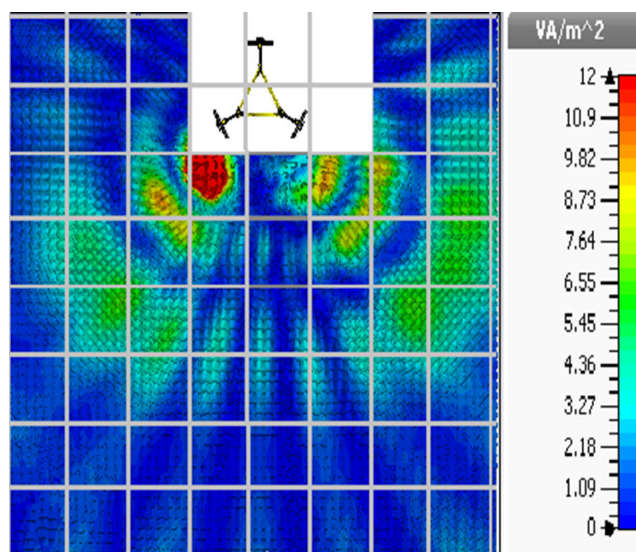

Fig. 11. Determination of safe distance in GSM1800 station based on environmental and occupational exposure limits

Figures 10 and 11 show the simulated power density in both stations. The color code has been adjusted such that the red areas indicate points where the occupational exposure limits are exceeded.

Figures 12 and 13 show the results of contour maps (contour lines) created by Surfer software. Figure 13 indicates the power density emission pattern in GSM1800 antenna station by both measurement and simulation. Comparing the two methods reveals that power density values in direct measurement were slightly higher than those in simulation, and this is attributed to the unstable near-fields in the vicinity of antennas. However, by distancing from the antenna, the instability, as well as the distance between measurement values and simulation values, decrease. Furthermore, the comparison between the two figures illustrates the significant compliance between simulation and measurement values. Figure 13 shows the contour lines of GSM900 antenna station. In that station, wave emission patterns around the antenna are slightly different; however, by distancing from the antenna, the difference had an increasing behavior. In Figure 13, due to the environmental scatterers, measured emission pattern is rather disordered as compared with simulated contours. Comparison of the measured and computational model-results at different distances from the antennas demonstrate their high compliance in far field distances. This matches with the results reported by [17], in which power density evaluation in different distances and antennas was conducted by both simulation and direct measurements. Computed Power density achieve compliance with direct measurement by distancing from the antennas [17]. Furthermore, all results of measurements follow standard limitations. Results of [5], an study on numerical calculations and direct measurement, revealed that theoretical methods can be reasonable for estimation of outdoor power density and electrical fields whereas indoor electrical fields do not have a high compliance due to their higher reverberation and related modeling complexities. Results of the present study also showed the effectiveness of power density estimation for the estimation of permissible limits around the antennas. Nevertheless, its validity depends on a low level of environmental reflectors, e.g. surrounding structures, fences, walls, metallic masts, etc. The estimation of the power density seems to be difficult when complicated environments such as indoor environments are to be considered. The results of GSM900 station demonstrate that after direct measurement, contour lines are affected by the existence of scatterers such as metal objects on the roofs. The power density measuring time can also affect the results such that longer measurement times can lead to the higher compliance of power densities obtained with less measuring errors. Other factors affecting the simulation efficiency are rather large volume of the computational domain and limitations in computational tools.

5- Conclusion

This study showed the verification of simulation methods for exposure assessment in simple GSM tower settings. Measurements of power densities were performed for an array of points near two different roof-based towers operating at 900 and 1800 MHz. Simulation of the towers provided similar contour maps of exposure and could be used to locate areas where exposure standards might be exceeded. Differences of about 10% existed between the measured and simulated values, which increased when measured points were close to scatterers on the placement area. Finally, although the results of this research suggest simulation as an exposure assessment tool, it cannot be a
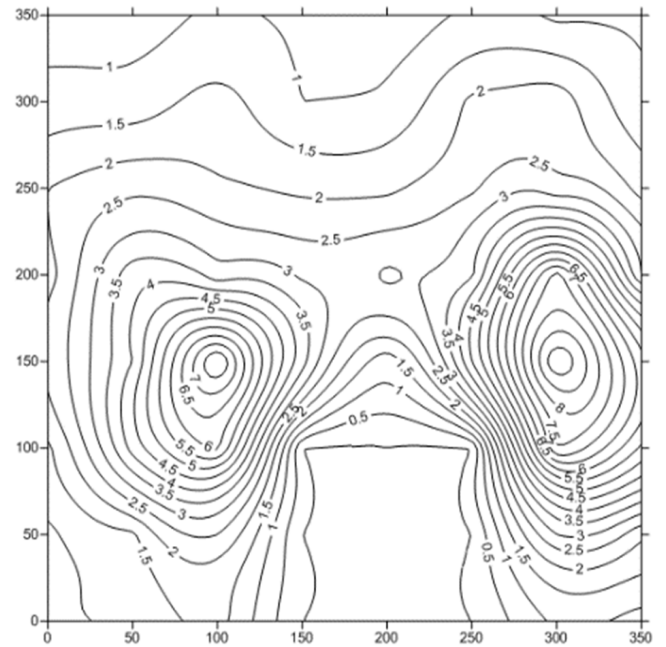
(1)
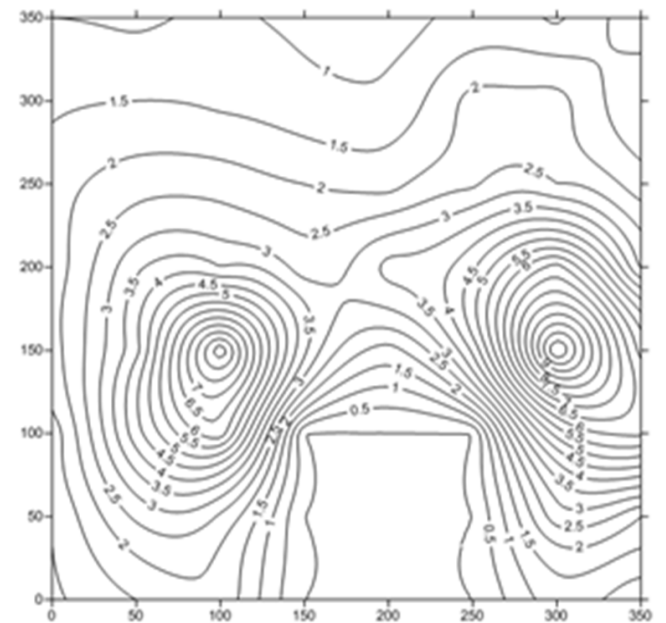
(2)

Fig. 12. Contour lines around GSM1800 antenna in both power density measurement (1) and simulation (2)
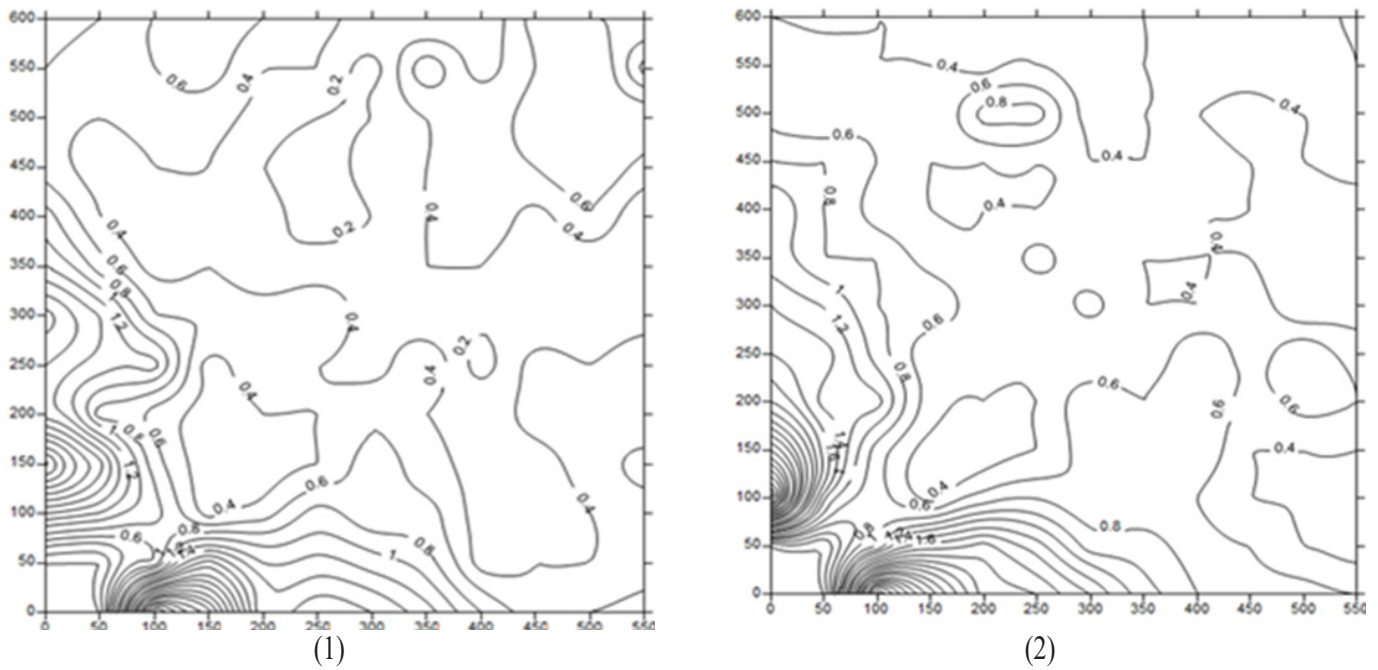
Fig. 13. Contour lines around GSM900 antenna in both power density measurement (1) and simulation (2)
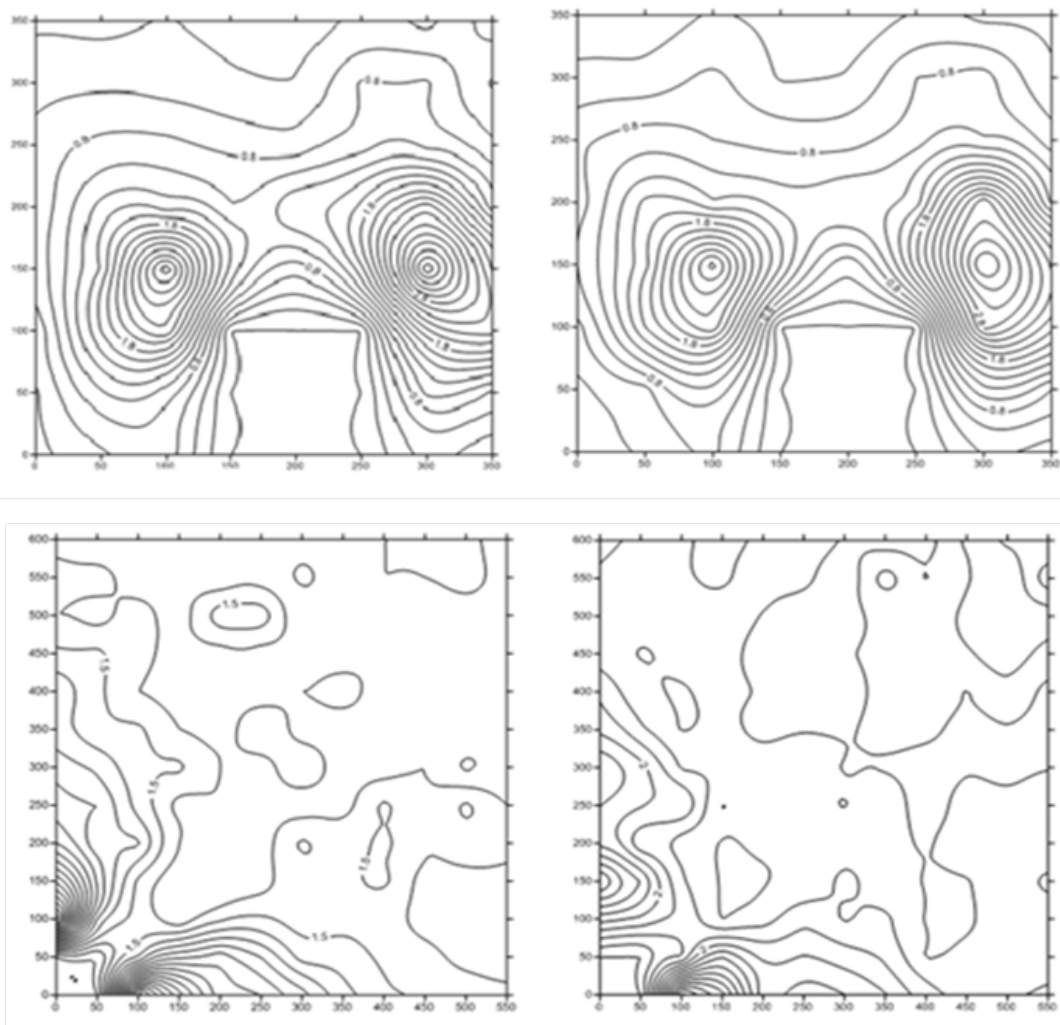

Fig. 14. Results of normalizing the X/X‾ in power density values

substitute for the measurement when available modeling data are insufficient, as regards the input power to the antennas, their working frequency, and structure.

REFERENCES

[1] P. Ushie, V.U. Nwankwo, A. Bolaji, O. Osahun, Measurement and Analysis of Radio-frequency Radiation Exposure Level from Different Mobile Base Transceiver Stations in Ajaokuta and Environs, Nigeria, arXiv preprint arXiv:1306.1475, (2013).

[2] P. Baltrėnas, R. Buckus, Indoor measurements of the power density close to mobile station antenna, (2011).

[3] Q.Q. He, W.C. Yang, Y.X. Hu, Accurate method to estimate EM radiation from a GSM base station, Progress In Electromagnetics Research M, 34 (2014) 19-27.

[4] M.A. Keow, S. Radiman, Assessment of radiofrequency/microwave radiation emitted by the antennas of rooftop-mounted mobile phone base stations, Radiation protection dosimetry, 121(2) (2005) 122-127.

[5] S. Miclaus, P. Bechet, Estimated and measured values of the radiofrequency radiation power density around cellular base stations, Romanian Journal of Physics, 52(3/4) (2007) 429.

[6] W. Suwansin, P. Phasukkit, C. Pintavirooj, A. Sanpanich, Analysis of heat transfer and specific absorption rate of electromagnetic field in human body at 915 MHz and 2.45 GHz with 3D finite element method, in: Biomedical Engineering International Conference (BMEiCON), 2012, IEEE, 2012, pp. 1-4.

[7] S. Banik, S. Bandyopadhyay, S. Ganguly, Bioeffects of microwave—a brief review, Bioresource technology, 87(2) (2003) 155-159.

[8] A. Khavanin, Nonthermal Effects of Radar Exposure on Human: A Review Article, Iranian Journal of Health, Safety and Environment, 1(1) (2014) 43-52.

[9] A. Vander Vorst, A. Rosen, Y. Kotsuka, RF/microwave interaction with biological tissues, John Wiley & Sons, 2006.

[10] T. Alanko, M. Hietanen, P. Von Nandelstadh, Occupational exposure to RF fields from base station antennas on rooftops, annals of telecommunications-annales des télécommunications, 63(1-2) (2008) 125-132.

[11] R. Kitchen, RF and microwave radiation safety handbook, Newnes, 2001.

[12] I.C.o.N.-I.R. Protection, Guidelines for limiting exposure to time-varying electric and magnetic fields (1 Hz to 100 kHz), Health physics, 99(6) (2010) 818-836.

[13] R.G. Sargent, Verification and validation of simulation models, in: Proceedings of the 37th conference on Winter simulation, winter simulation conference, 2005, pp. 130-143.

[14] Y. Alfadhl, Numerical evaluations on the interaction of electromagnetic fields with animals and with biological tissues, University of London, 2006.

[15] Roof Top guide 122-A, n.kouhestani cartographer2015.

[16] Roof Top guide 195-A n.kouhestani, cartographer2015

[17] P. Gajšek, D. šimunic, Occupational exposure to base stations—compliance with EU Directive 2004/40/EC, International Journal of Occupational Safety and Ergonomics, 12(2) (2006) 187-194.